CERN-ACC-2022-0001
rogelio.tomas@cern.ch

HL-LHC Run 4 proton operational scenario

G. Arduini, P. Baudrenghien, O. Brüning, R. Bruce, X. Buffat, R. Calaga, R. De Maria, J. Dilly, I. Efthymiopoulos, M. Giovannozzi, P.D. Hermes, G. Iadarola, S. Kostoglou, B. Lindström, E.H. Maclean, E. Métral, N. Mounet, Y. Papaphilippou, T.H.B. Persson, T. Pugnat, S. Redaelli, G. Sterbini, H. Timko, R. Tomás, F. Van der Veken, J. Wenninger, and M. Zerlauth,
CERN, Geneva, Switzerland.

Abstract

Following new findings in beam dynamics and the latest HL-LHC project decisions, an operational scenario has been developed for the first HL-LHC run, Run 4. This new scenario is presented in this document along with the motivations for the proposed changes and performance estimates.

Geneva, Switzerland
June 29, 2022

Contents

1 Introduction

The HL-LHC baseline and ultimate scenarios were presented in Ref. [1], describing the beam and machine parameters throughout the operational cycle. Since then, various devices have been added or removed from the HL-LHC baseline and new considerations and constraints have significantly changed the machine configuration. The main items are briefly described as follows:

- **Postpone the installation of sextupoles in the dispersion suppressor to Long Shutdown 4 (LS4)**. It has been verified [2, 3] that beam lifetime due to DA without these sextupoles is acceptable for optics with $\beta^* \geq 20$ cm in IP1 & IP5, which is the current assumption for Run 4. However, at $\beta^* = 15$ cm, foreseen for Run 5 operation, these sextupoles will be needed [4].
- **Luminosity limitation to 2.5×10^{34} cm^{-2}s^{-1} at the start of the fill**. This limitation is introduced to allow triplet cryogenics to adapt to the heat-load coming from the luminosity debris [5, 6]. Luminosity should first stay for 10 minutes at 2.5×10^{34} cm^{-2}s^{-1} and then it can be ramped up to 5×10^{34} cm^{-2}s^{-1} in another 10 minutes.
- **Partial upgrade of the secondary CFC collimators, all but two (per beam) being replaced with low-impedance collimators** [7]. This decision was driven by cost considerations, with the drawback of a small increase of the machine impedance. The low-impedance collimators are Mo-coated MoGr collimators.
- **Increase of primary collimator gap from 6.7 σ to 8.5 σ at top energy**. To ensure beam stability during the collision adjustment process [8], the impedance of the collimator system is reduced by increasing the collimators gaps. The new settings for the secondary and tertiary collimators are presented below.
- **Positive octupole polarity**. This choice of polarity does not require to increase the β functions in the arc octupoles ($r_{ATS} = 1$) to stabilize the beams at the start of the physics fill [8]. Moreover, it features a significantly larger dynamic aperture (DA) at injection for the nominal working point above the diagonal [9, 10].
- **Cancellation of the installation of 11 T dipoles in LS2**. The earliest possible date of installation of these dipoles and the IR7 TCLDs seems to be LS4, due to manpower limitations [11]. Therefore Run 4 will most likely happen without IR7 TCLDs and 11 T dipoles.
- **Crab cavity (CC) noise**. The expected CC phase and amplitude noise induce a transverse emittance growth larger than expected in [11]. This is now accounted for during physics in Run 4. One mitigation would be a dedicated

feedback, based on a new BPM and acting on the CC voltage [12]. This option is being considered, but needs further studies. Another mitigation would consist in operating with slightly flat optics, i.e. $\beta_x^* \neq \beta_y^*$ [13].

- **Full Remote Alignment System (FRAS) included in the HL-LHC baseline** [14]. This system allows IR elements to be moved, potentially freeing aperture and orbit correctors strength, which was initially assumed to be reserved for shifting transversely the IP or to cope with ground motion.
- **Hollow Electron Lens (HEL) included in the HL-LHC baseline** [15]. The HEL is an advanced tool for active control of diffusion speed of halo particles which will serve to mitigate losses from fast processes.
- **Reduction of β^* for LHCb from 3 m to 1.5 m** [16]. This is needed to increase the integrated luminosity in LHCb thanks to a longer leveling time.
- **Rotation of the external crossing angle in IR8 from horizontal to vertical at top energy** [16].
- **Upgrade of the eight main dipoles power converters from class 1 to class 0.5** [17]. This is needed to improve tune ripple and β^* control [18].
- **Introduction of crystal collimation for ions**. These devices have to be compatible with proton operation in terms of impedance and e-cloud effects, although they are only used in operation with ions.

Run 4 is foreseen to start in mid 2027, with the beam commissioning of the new hardware and a performance ramp-up required to master the higher bunch intensity, new devices such as the HEL and CCs, and to ensure the proper optics control [18]. The baseline plan for the HL-LHC ramp-up is given in Table 1 and Fig. 1, allowing to integrate above 550 fb^{-1} during Run 4. In 2030, with 160 days of physics, the integrated luminosity is expected to be in excess of 240 fb^{-1}.

The bunch intensity in the first years of HL-LHC operation should match the one achieved in Run 3, for now 1.7×10^{11} ppb is taken until new estimates are available. The crossing angle in these first years has been chosen as 450 μm to provide sufficient DA at start of levelling, see Section 7.1. Reducing the crossing angle during the fill down to Run 3 values gives similar integrated luminosity as with constant crossing angle at 380 μm. Further to this it is also assumed that the tail population would not differ significantly from Run 3, allowing to experiment with HEL and CCs in 2027 and 2028, before putting them in operation in 2029. HEL commissioning could attract higher priority in case the machine would experience limitations related to the halo population. Concerning non-linear optics commissioning it is verified that IR decapolar and dodecapolar corrections are not needed in the first years of operation [19].

The relevant beam and machine parameters for Run 4 are presented in the following sections and, unless stated otherwise, we focus on the last year of Run 4

Table 1: Protons per bunch (ppb), virtual luminosity (calculated with $\beta^* = \beta^*_{\text{end}}$), full crossing angle ($\theta$) and β^* targets in the HL-LHC luminosity ramp-up years. A normalised emittance, $\varepsilon_n = \varepsilon\gamma$ with $\gamma = E/m_p$, of $\varepsilon_n = 2.5$ μm is assumed for all years. β^*_{start} and β^*_{end} correspond to the β-function at the start and at the end of the physics fill. β^*_{start} is defined to deliver 2.5×10^{34} cm^{-2}s^{-1} at the start of the fill to meet the requests from cryogenics. The Ultimate scenario is highlighted in yellow.

Year	ppb [10^{11}]	Virtual lumi. [10^{34}cm^{-2}s^{-1}]	Days in physics	θ [μrad]	β^*_{start} [cm]	β^*_{end} [cm]	HEL and CC	Max. PU
2027	1.7	3.5	30	450	50	30	exp	92
2028	1.7	3.5	120	450	50	30	exp	92
2029	2.2	11.3	140	500	100	25	on	132
2030	2.2	13.5	160	500	100	20	on	132
2031			Long shutdown 4					
2032	2.2	13.5	170	500	100	20	on	132
2033	2.2	16.9	200	500	100	15	on	132
2033	2.2	16.9	200	500	100	15	on	200

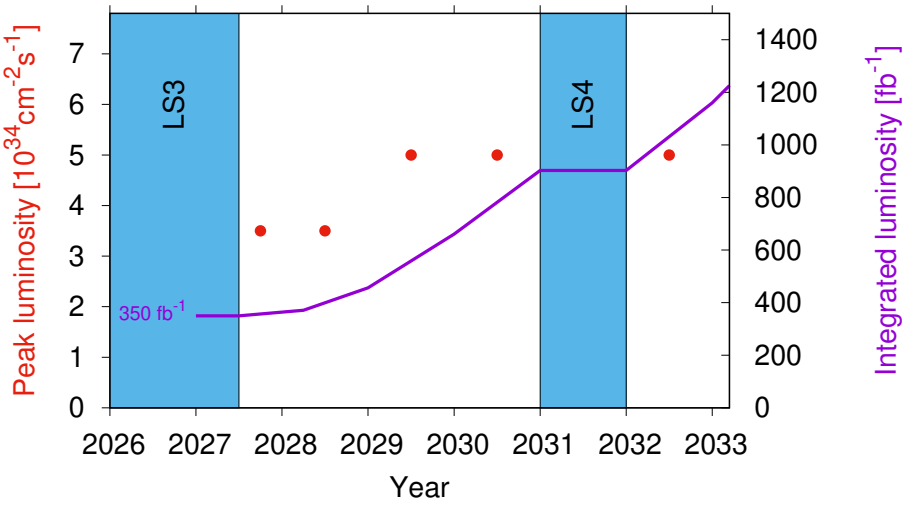

Figure 1: Peak and integrated luminosity during Run 4, assuming an integrated luminosity of 350 fb^{-1} by the end of Run 3.

Table 2: Breakdown of the minimum turn-around and physics fill times for Run 4.

Phase	Time duration [minutes]	Accumulated time [minutes]
Ramp-down	40	40
Pre-injection set-up	15	55
Set-up with beam	15	70
Nominal injection	30	100
Prepare ramp	5	105
Ramp & Squeeze	25	130
Flat-top	5	135
Collision adjustment	10	145
First luminosity plateau	10	155
Luminosity ramp up	10	165
Luminosity levelling	305	470
Luminosity decay	115	585

operation. Section 2 gives a global overview of the machine cycle, describing the turn-around time, the filling schemes, and the parameters that remain constant during the entire cycle. Section 3 describes the current optics and the level of accuracy required for most of the key optics parameters. Section 4 contains the beam and machine parameters at the end of the injection process. Section 5 gives the beam and machine parameters at top energy, right after the energy ramp. Section 6 describes the process of bringing the beams into collision, named as collision adjustment process. Section 7 contains the parameters at the start of the nominal luminosity leveling of 5×10^{34} cm^{-2}s^{-1}. Section 8 describes the end of the nominal luminosity levelling. Section 9 presents the Run 4 performance in case there would be an intensity limitation in the range between 1.8×10^{11} ppb and 2.3×10^{11} ppb at injection. Section 10 gives analytical equations for the amplitude detuning and second-order chromaticities induced by the Landau octupoles as a function of energy, octupole current, and ATS factor r_{ATS}.

2 The physics cycle

The turn-around time is defined as the time between the dump of the physics beams and restart of the next physics fill. This time plays a fundamental role in the accelerator performance, and strongly influences the length of the optimum physics fill. The different stages during the turn-around and the physics fill are given in Table 2 together with their corresponding lengths.

Table 3: Filling schemes. Quantitative information on the number of pairs of various IP1&5 and IP8 collision configurations is given.

Filling pattern	Standard	BCMS
Maximum bunches per beam	2760	2744
Colliding pairs in IP1/2/5/8	2748/2492/2748/2574	2736/2246/2736/2370
Non-colliding pairs in IP1&5	12	8
Pairs colliding in IP1&5&8	2376	2017
Pairs colliding in IP1&5 with one bunch colliding in IP8	372	690
Pairs colliding only in IP1&5	0	29

Figure 2 shows a schematic view of the Run 4 operational cycle with key beam parameters and luminosity. The abrupt jumps in bunch intensity and emittances during the collision adjustment process, just before 2.5 h, correspond to the intensity loss and emittance growth budgets assigned for the interval between injection and the start of collisions, however they are here pessimistically lumped when collisions are established. The slow horizontal emittance growth at injection is due to intra-beam scattering (IBS). The luminosity starts with a step at $2.5 \times 10^{34}\text{cm}^{-2}\text{s}^{-1}$ followed by a linear ramp to meet the cryogenic requests. The bunch intensity and emittance evolution during physics include burn-off, IBS, synchrotron radiation (SR) damping, and emittance growth from CC noise. Emittance growth from luminosity burn-off has a small effect on the HL-LHC integrated luminosity of about 1% [20], not included in this report, and should be further studied for more accurate predictions.

Two filling schemes are considered for operation in HL-LHC: Standard and BCMS. The collision patterns for these schemes are described in Table 3 [21, 22]. Beam and machine parameters for these two filling schemes are reported in the coming sections. The 12 bunches that do not collide in IP1&5, called witness bunches, are assumed to have a factor 4 lower brightness than the nominal bunches, i.e. 1.1×10^{11} ppb within a normalised transverse emittance of 5 μm in both planes, to reduce the strength of Landau octupoles during physics [23]. The practical aspects of this assumption are discussed in Section 2.1. Quantitative information on the pairs colliding in the various IP1, IP5 and IP8 configurations is given on Table 3 as it is relevant for burn-off calculations and stability. Alternative filling schemes can be proposed to further reduce the strength of Landau octupoles in physics by optimising the collisions of the witness bunches in IP2 & IP8 [24].

Table 4 lists parameters that are constant during the entire cycle, which are mostly related to RF, damper, and CCs. The CC RF noise parameters were last

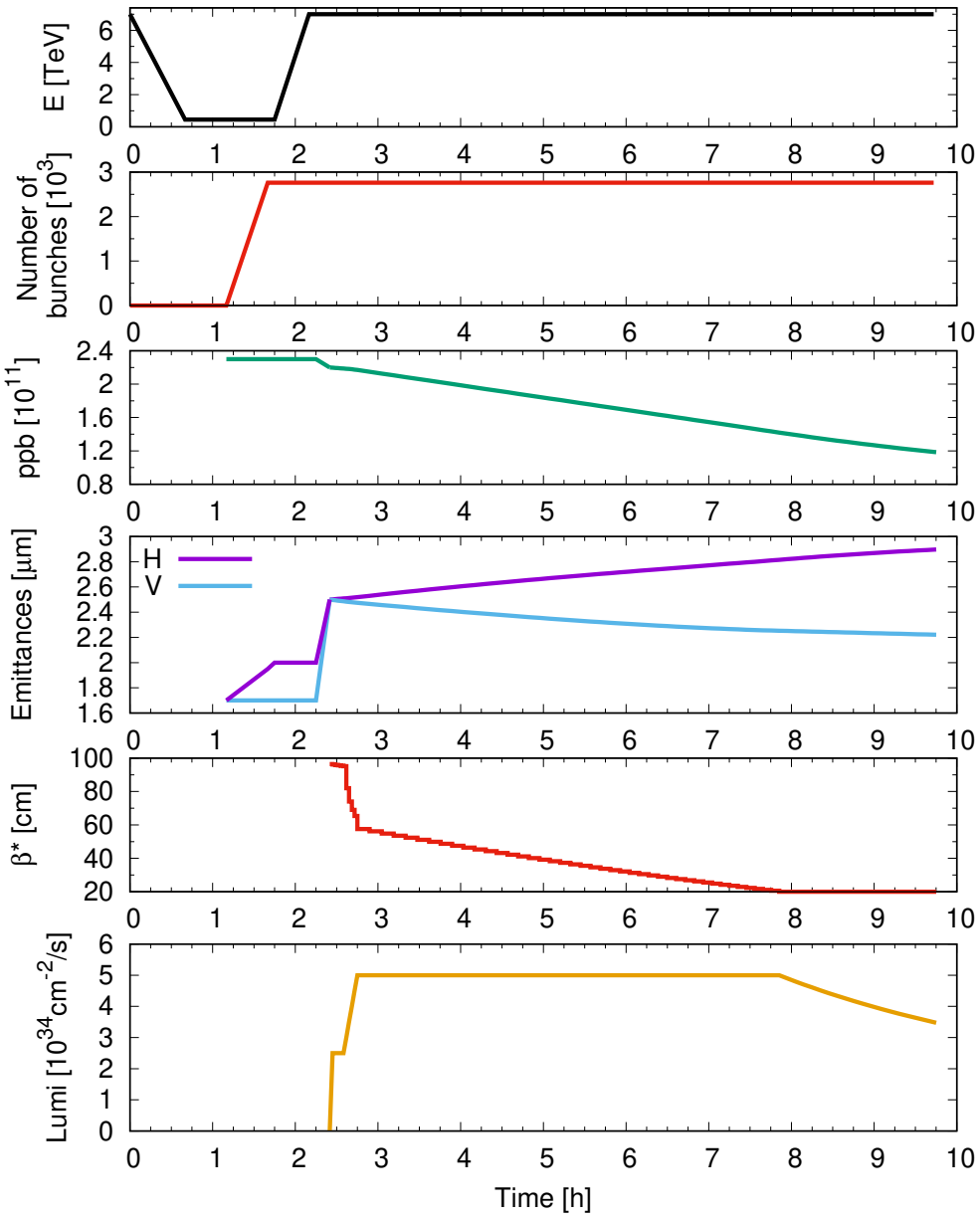

Figure 2: A schematic view of the Run 4 HL-LHC physics cycle showing magnetic cycle, number of bunches, protons per bunch (ppb), transverse emittances (BCMS case), and luminosity (top to bottom) versus time until the beam dump.

Table 4: Main RF parameters including CCs and damper.

Harmonic number	35640
Revolution frequency [kHz]	11.2455
Main RF and CC frequency [MHz]	400.79
Transition gamma	54
Length of the abort (no beam) gap [μs]	3
Maximum noise from damper pick-up electronics [μm]	0.2
CC: max. Left/Right relative amplitude error [%]	1
CC: phase noise (white noise equivalent) [10^{-5}rad]	2.7
CC: relative amplitude noise (white noise equivalent) [10^{-5}]	2.7*
CC: transverse emittance blow-up @ β^*=15cm [%]	<5.2

*When cavities are with opposite phases with low voltage, the amplitude noise could be reduced.

updated in [25]. The resulting emittance growth given on the table is estimated at $\beta^* = 15$ cm. For larger β^* the emittance growth is reduced according to the scaling $1/\beta^*$.

2.1 Witness bunches

The intermediate bunch train, consisting of 6 to 12 bunches, was introduced in the LHC filling schemes during Run 1 to avoid a large intensity and stored energy steps from one circulating probe bunch to trains of 288 bunches with nominal intensity ($> 10^{11}$ protons). The stored energy of such a train at 450 GeV corresponds roughly to the threshold (10^{12} protons) where damage by beam of a Copper vacuum chamber becomes possible in case of uncontrolled beam loss.

Since Run 1 the typical LHC filling sequence consists of the following three steps:

- Injection of a probe bunch to setup the machine at injection (tunes, chromaticities and orbits). If necessary the probe bunches are dumped and re-injected multiple times.
- With one probe bunch circulating in the ring, at least one intermediate bunch train is injected. If trajectory excursions and beam losses are adequate, the LHC shift crew proceeds to the next step, else it may decide to perform beam steering and tuning in the injectors (for example transverse scrapping in the SPS) by injecting a sequence of intermediate trains. At the end of the tuning the intermediate trains are dumped, and the filling sequence is restarted from a probe bunch.
- Filling the long trains that are injected one after the other. The probe bunch is eliminated during the filling process either by cleaning out using the in-

jection cleaning function of the transverse damper or by overinjecting during one of the train injections.

The LHC Software Interlock System enforces the injection of the intermediate intensity train by comparing the circulating beam intensity in each LHC ring with the beam intensity in the SPS just before the start of the SPS energy ramp. It will block injection of nominal trains if the circulating beam intensity in the LHC is too low (absence of intermediate train).

To be able to use the intermediate intensity train for beam steering and setup as described above, the bunch characteristics (intensity, emittance and tails) must be as similar as possible to the nominal beam injections. In that case losses may for example be scaled from intermediate train to nominal train length to evaluate if the nominal trains may be injected without risk of beam dump on beam losses. Beam dumps on beam losses above threhold are the main reason for aborts of the injection sequence.

For Run 3 two improvements are foreseen for injection steering and beam losses.

- Some of the highest beam loss signals are generated by showers due to scrapping on transfer line collimators. Those showers hit the LHC ring BLMs from the outside and represent an external cross-talk signal (fake loss) that occurs on a single pass during the transfer. The BLM system firmware has been upgraded during LS2 with a "signal blinding" option around the time of injection. When it is activated the loss occuring in the turns around injection are ignored. This feature may be activated for selected BLMs to render the LHC injection process less sensitive to single pass tail scrapping.
- For safety reasons steering of the transfer lines was so far only performed on intermediate trains (enforced by procedure). In Run 3 it is planned to allow gentle steering also with the nominal injections.

If applied successfully those two changes could help loosening the requirements on intensity and tails between intermdiate and nominal trains.

Finally it is also possible to envisage to blow up the transverse emittance of the intermediate train with the transverse damper just before starting the ramp to increase the instability threshold for those trains at high energy when they are not colliding head-on in any IP.

3 Optics control parameters

This document uses HL-LHC optics version 1.5 for Run 4 [26]. To guarantee beam stability and sufficient beam lifetime throughout the entire cycle, it is fundamental to control some key optics parameters with high accuracy [18, 27, 28].

Table 5: Optics control parameters throughout the magnetic cycle. δ_p is the relative energy deviation of a particle. σ^* represents the IP beam size and σ_δ the rms relative momentum spread.

Residual coupling (without beam-beam effects)	0.001
Required tune control	0.001
Minimum tune separation (incl. collision adjustment process)	0.005
Chromaticity Q' $(\mathrm{d}Q/\mathrm{d}\delta_p)$	+15
Chromaticity control $\Delta Q'$	± 5
Max. dispersion at the IP	$0.14\sigma^*/\sigma_\delta$
Max. beta-beating at IP [%]	2.5

These are listed in Table 5. In particular, for coupling at injection it is observed that a closest tune approach of 0.003 yields poorer DA than the current 0.001 target [10]. Coupling at the top energy could drift during the run due to, e.g. ground motion. To control accurately the coupling during the physics process a dedicated filling scheme with few non-colliding bunches (in any IR) should be used at most every two weeks [28]. The maximum IP dispersion tolerance is set to avoid beam size increase larger than 1%. For example at $\beta^* = 20$ cm and $\varepsilon_n = 2.5$ μm, σ^* is about 8 μm and the related dispersion tolerance is about 1 cm.

4 Injection

The parameters of the beams coming from the injectors are described in [1]. During the injection process, the beam emittances suffer a blow-up due to IBS [29]. Beam parameters after the injection process are given in Table 6. In the longitudinal plane, the density follows a q-Gaussian distribution as described in Ref. [1]. The full width at half maximum $FWHM$ of such a q-Gaussian distribution with rms value σ_{q-G} is given by

$$FWHM = 4\sqrt{2-2^{3/5}}\sigma_{q-G}\,. \tag{1}$$

From longitudinal stability considerations, two longitudinal beam distributions are regarded as equivalent when they have equal $FWHM$. Therefore the Gaussian distribution equivalent to a q-Gaussian with rms σ_{q-G} has an rms σ_G given by

$$\sigma_G = \sqrt{\frac{4-2^{8/5}}{\ln 2}}\;\sigma_{q-G}\,. \tag{2}$$

Concerning transverse stability, recent studies for the LHC [30] show that the best Gaussian approximation to a q-Gaussian longitudinal distribution is with a

Table 6: **Injection:** Beam and RF parameters including CCs and damper. The beam parameters correspond to the end of injection process and before the energy ramp, taking into account IBS growth.

	Standard	BCMS
Energy [TeV]	0.45	
ppb [10^{11}]	2.3	
Particles per beam [10^{14}]	6.3	6.3
Beam current [A]	1.1	1.1
ε_n (H/V) [μm]	2.3/2.1	2.0/1.7
ε_L [eVs]	0.63	0.65
RMS bunch length (q-Gaussian) [cm]	8.3	8.4
RMS energy spread (q-Gaussian) [10^{-4}]	3.3	3.3
IBS growth-times (H/V/L) [h]	4.5/145.5/2.6	3.2/94.8/2.1
Total RF voltage [MV]	8*	
Cavity detuning used	Half-detuning	
Synchrotron frequency [Hz]	66	
Bucket area [eVs]	1.38	
Bucket half height ($\Delta E/E$) [10^{-4}]	9.65	
CC voltage per cavity [MV]	0.25	
CC phase between cavities on same IP side [deg]	180	
CC total voltage [MV]	0	
Transverse damper damping time [turns]	10	
Transverse damper bandwidth [MHz]	20	

*Optimum voltage is under investigation.

rms value of σ_{q-G}. This approach was used to compute the octupole settings in this report [31]; this approximation might be slightly pessimistic and will be reviewed in the future.

Concerning DA with beam-beam, first studies have shown only a weak dependency of the DA on the longitudinal distribution [32]. The above mentioned equivalence between q-Gaussian and Gaussian distributions is assumed in this report.

The injection optics parameters are given in Table 7. The crossing angle in IP2 and IP8 is the sum of an external crossing angle bump and an "internal" spectrometer compensation bump (which is inversely proportional to the energy) and it depends on the spectrometer polarity. The values quoted in the table correspond to the sum of the two, noting that one configuration provides a minimum beam-beam long-range normalised separation. The external bump extends over the triplet and

D1 and D2 magnets. The internal spectrometer compensation bump extends only over the long drift space between the two Q1 quadrupoles left and right from the IP. The convention for the spectrometer polarity sign is that it is positive for a negative sign of the crossing angle [33].

IP2 and IP8 have, respectively, small horizontal and vertical crossing angle components due the fact that the spectrometer and the corresponding compensator magnets are aligned to the horizontal plane of the experimental hall, while the LHC tunnel is tilted with respect to that plane [34]. The sign is correlated with the sign of the internal crossing angle. IP2 and IP8 also feature an external parallel angle (same sign and size for both beams) in the separation plane to optimise aperture.

Figure 3 shows the DA at injection. For the DA studies, an initial distribution of particles that forms a polar grid in the initial configuration space, consisting of 5 angles and amplitudes extending up to 10 σ, are tracked for 10^6 turns, corresponding to a duration of approximately 90 seconds of the accelerator's operation. Longitudinally, the particles are placed at a momentum offset corresponding to 3/4 of the RF bucket height and the simulations include the effect of the synchrotron motion. Important non-linearities induced by the chromaticity sextupoles, the Landau octupoles and long-range beam-beam encounters are considered, while magnetic field errors are not treated in the present report. The weak-strong approximation is used to treat beam-beam effects as the charge distribution of the opposite beam is considered unperturbed. The main observable is the minimum DA across the angles that form the initial distribution. The 6 σ target is reached for few locations near the injection operational working point $Q_{x,y} = 62.27,\ 60.295$, losing about 0.5 σ of DA for tune changes of 0.005. If needed, it seems possible to increase DA by optimising the IP1-5 phase advance and reducing the crossing angle [10].

Collimator, injection protection, and HEL settings are reported in Table 8. The injection protection devices are moved to the flat-top settings, see Table 11, before the energy ramp. The transverse damper gain is also reduced to the flat-top setting (see Table 9) before the energy ramp.

5 Flat-top

The flat-top energy is reached after the combined energy ramp and β^* squeeze to 1 m. This involves changing the optics, orbit, RF, collimation, and HEL during the energy ramp. The following steps should be performed sequentially either after reaching the top energy or towards the end of the combined ramp & squeeze:

- Rotation of the plane of the crossing angle in LHCb from horizontal to vertical.

Table 7: **Injection:** Optics and crossing scheme parameters. All separations and crossing angles correspond to the half of the value seen between the two beams. The crossing angle and separation refer to Beam 1 if not specified otherwise. For Beam 2 the crossing angles and the separations have the opposite sign using the MAD-X Beam 1/Beam 2 reference system conventions. The half-separations in σ are estimated for the normalised emittance of 2.5 μm.

Optics filename	opt_inj_6000
β^* [m] in IP1/2/5/8	6.0/10.0/6.0/10.0
ATS Telescopic factor r_{ATS}	1.0
Tunes (H/V)	62.27/60.295
Crossing angle at IP1 (ATLAS) [µrad]	500[e] (H)
Separation in separation plane at IP1 (ATLAS) [mm/σ]	2.0/11.3[g] (V)
Separation in crossing plane at IP1 (ATLAS) [mm]	0
External crossing angle at IP2 (ALICE) [µrad]	-170[$] (V)
Crossing angle at IP2 (ALICE) [µrad]	$\mp$4.5 (H) $\mp$1089-170 (V)
Separation in separation plane at IP2 (ALICE) [mm/σ]	3.5/15.3[i]
Separation in crossing plane at IP2 (ALICE) [mm]	0 (V)
External parallel angle at IP2 (ALICE) [µrad]	-40 (H)
Crossing angle at IP5 (CMS) [µrad]	500[$] (V)
Separation in separation plane at IP5 (CMS) [mm/σ]	2.0/11.3[$] (H)
Separation in crossing plane at IP5 (CMS) [mm]	0[g] (V)
External crossing angle at IP8 (LHCb) [µrad]	-170 (H)
Crossing angle at IP8 (LHCb) [µrad]	-170 ∓ 2100(H) $\mp$28 (V)
Separation in separation plane at IP8 (LHCb) [mm/σ]	$-3.5/-15.3$[i] (V)
External parallel angle at IP8 (LHCb) [µrad]	-40 (V)
Min. Landau octupole current (LOF) [A] required for beam stability (Standard/BCMS)	36[j] / 45[j]
RMS betatron tune spread[k] [10^{-3}]	0.6
Residual detuning with amplitude due to lattice non-linearities [35] [Amps-equiv. in LOF]	0-3

[e] In the horizontal plane the sign of the crossing angle is defined by the geometry.

[g] It is preferred to have the same sign of the crossing angle to reduce the orbit corrector strength.

[$] The other sign is possible.

[i] The other sign is possible, but the parallel angle and separation are correlated for the same IP.

[j] Requirement for the bunch with lowest emittance (2.1 μm for Standard and 1.7 μm for BCMS), scaled from 2018 operation, neglecting the impact of the higher bunch intensity, which should be beneficial).

[k] Sources of detuning taken into account: Chromatic sextupoles, Landau octupoles and long-range beam-beam interactions.

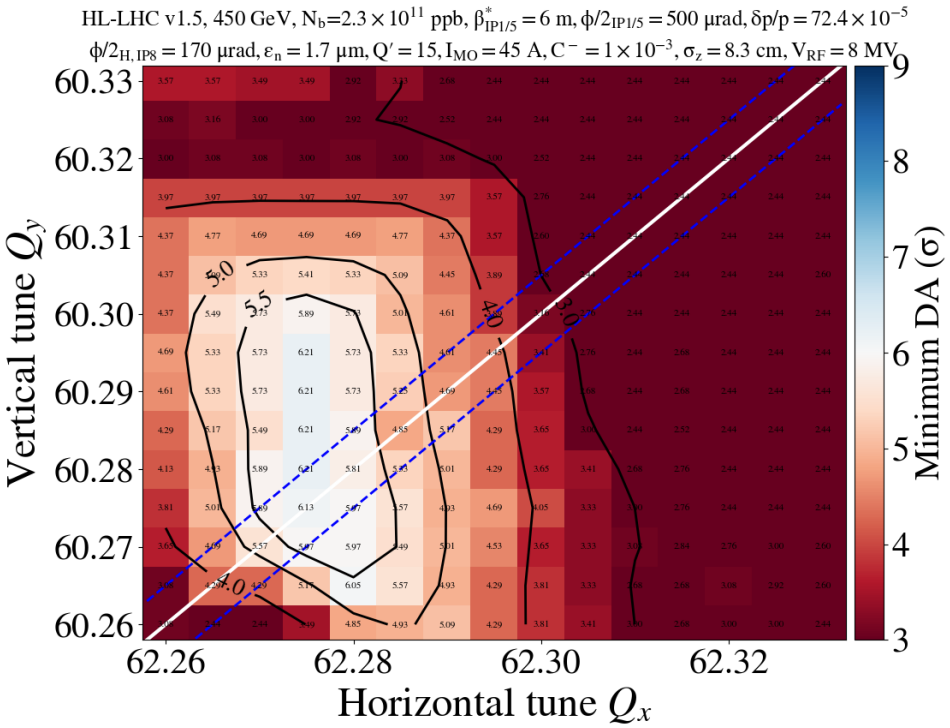

Figure 3: DA at injection versus horizontal and vertical tunes.

Table 8: **Injection:** Collimation, injection protection and HEL settings. All collimator and injection protection settings correspond to the half-gap. Settings in σ correspond to a normalised emittance of 2.5μm. Both beams have the same value unless specified otherwise, blue for Beam 1 and red for Beam 2.

TCP/TCPM IR7 [σ]	6.7
TCSPM/TCSG IR7 [σ]	7.9
TCLA IR7 [σ]	11.8
TCLD IR2 [mm]	20
TCP IR3 [σ]	9.5
TCSG IR3 [σ]	11.0
TCLA IR3 [σ]	11.8
TCSP IR6 [σ]	8.3
TCSP IR6 (Beam 1 / Beam 2) [mm]	14.0 / 14.0
TCDQ IR6 [σ]	9.5
TCDQ IR6 (Beam 1 / Beam 2) [mm]	15.7 / 15.7
TCT H4-V4-H6-V6 IR1&5 [σ]	15.4-15.4-15.4-15.4
TCT H4-V4-H6-V6 IR1/5 [mm]	17.9-13.6-13.9-8.8 / 18.0-13.6-13.9-8.8 18.0-13.4-13.9-8.8 / 18.0-13.4-13.9-8.7
TCL4-5-6 IR1&5	parking
TCL4-5-6 IR1/5 [mm]	35-25-25 / 35-25-25
TCT IR2 [σ]	15.4
TCT IR8 [σ]	15.4
TDIS IR2 [mm]	3.9
TDIS IR8 [mm]	3.8
TCDD IR2 [mm]	24
TCLIA IR2 [mm]	6.5
TCLIA IR8 [mm]	6.6
TCLIB IR2 [mm]	4.2
TCLIB IR8 [mm]	2.8
Protected aperture [σ]	12.6
HEL e^- beam current [A]	0

Table 9: **Flat-top:** Beam and RF parameters including the CCs and damper.

	Standard	BCMS
Energy [TeV]	7	
ppb [10^{11}]	2.3	
Particles per beam [10^{14}]	6.3	6.3
Beam current [A]	1.1	1.1
ε_n (H/V) [μm]	2.3/2.1	2.0/1.7
ε_L [eVs]	3.03	
RMS bunch length (q-Gaussian) [cm]	7.61	
RMS energy spread (q-Gaussian) [10^{-4}]	1.1	
IBS growth-times (H/V/L) [h]	14.8/218.6/ 15.0	10.4/142.0/ 12.0
Damping times from SR (H/V/L) [h]	51.7/51.7/25.9	
Power loss due to SR (per arc cell) [W/m/beam]	0.34	
Total RF voltage [MV]	16	
Cavity detuning used	Full detuning	
Peak-to-peak RF phase [ps]	-53 to 49	-44 to 42
Synchrotron frequency [Hz]	23.8	
Bucket area [eVs]	7.63	
Bucket half height ($\Delta E/E$) [10^{-4}]	3.43	
CC voltage per cavity [MV]	0.25	
CC phase between cavities on same IP side [deg]	180	
CC total voltage [MV]	0	
Transverse damper damping time [turns]	50	
Transverse damper bandwidth [MHz]	20	

- Tune change from injection to collision values.

Depending on the need for tail depletion, it is also planned to switch on the HEL, either before the end of the ramp, e.g. at 5 TeV, or at the flat-top energy [15].

The main beam and RF parameters at the end of this process are listed in Table 9. The RF phase modulation is due to the operation in full detuning mode.

Table 10 shows the optics parameters at flat-top. The DA at flat-top is significantly larger than at injection or after having put beams in collision.

Table 11 shows the collimation, injection protection, and HEL settings at flat-top. Collimator settings in σ units are typically scaled linearly with the γ function during the energy ramp from the injection values of Table 8 to the flat-top values of Table 11 [38]. Collimator gap values and central position follow also the changes of local beta functions and orbit, respectively. After the injection is completed the

Table 10: **Flat-top:** Optics and crossing scheme parameters. All separations and crossing angles correspond to half of the full value between the two beams. The crossing angle and separation refer to Beam 1 if not specified otherwise. For Beam 2 the crossing angles and the separations have the opposite sign using the MAD-X Beam 1/Beam 2 reference system conventions. The half-separations in σ are estimated for the normalised emittance of 2.5μm.

Optics filename	opt_flattop_1000
β^* [m] in IP1/2/5/8	1.0/10.0/1.0/1.5
ATS Telescopic factor r_{ATS}	1.0
Tunes (H/V)	62.317/60.322
Crossing angle at IP1 (ATLAS) [µrad]	250[e] (H)
Separation in separation plane at IP1 (ATLAS) [mm/σ]	0.85/46[g] (V)
Separation in crossing plane at IP1 (ATLAS) [mm/σ]	0.075/4[g] (H)
External crossing angle at IP2 (ALICE) [µrad]	-170[$] (V)
Crossing angle at IP2 (ALICE) [µrad]	$\mp$0.3 (H) $\mp$70-170 (V)
Separation in separation plane at IP2 (ALICE) [mm/σ]	1.4/24[i]
Separation in crossing plane at IP2 (ALICE) [mm]	0 (V)
External parallel angle at IP2 (ALICE) [µrad]	0 (H)
Crossing angle at IP5 (CMS) [µrad]	250[$] (V)
Separation in separation plane at IP5 (CMS) [mm/σ]	0.85/46[g] (H)
Separation in crossing plane at IP5 (CMS) [mm]	0.075/4 (V)
External crossing angle at IP8 (LHCb) [µrad]	170 (V)
Crossing angle at IP8 (LHCb) [µrad]	$\mp$135 (H) $+170\mp1.8$ (V)
Separation in separation plane at IP8 (LHCb) [mm/σ]	1.0/45[i] (H)
External parallel angle at IP8 (LHCb) [µrad]	0 (V)
Min. Landau octupole current (LOF) [A] required for beam stability (Standard/BCMS)	380 / 460
RMS betatron tune spread[k] (min/max) [10^{-3}]	0.03 / 0.04
Residual detuning with amplitude due to lattice non-linearities [Amps-equiv. in LOF]	6

[e] In the horizontal plane the sign of the crossing angle is defined by the geometry.

[g] The other sign is possible. In the separation plane it is not correlated with other choices. In the crossing plane the same sign of the crossing angle is preferred for orbit corrector strengths.

[$] The other sign is possible.

[i] The other sign is possible but the parallel angle and separation are correlated for the same IP.

[k] Sources of detuning taken into account: Chromatic sextupoles, Landau octupoles and long-range beam-beam interactions

TDIS in IR2 and IR8 are retracted to the fully open position of 55 mm.

6 Collision adjustment process

During the collision adjustment process, the separation orbit bumps are reduced to provide the levelled luminosities as given in Table 12. In ATLAS and CMS the luminosity is first levelled at 2.5×10^{34} cm^{-2}s^{-1} for a short period as dictated by the cryogenic system. The collision adjustment process is one of the most critical phases from the point of view of beam stability and beam lifetime (related to DA). Crab cavities are assumed to be off or counter-phased during the collision adjustment process, to be ramped up during physics. This has the advantage that the collision adjustment process remains unchanged independently of the availability of CCs, which can be ramped up in a few minutes.

During the collision adjustment process, the following sequence of events occurs [8]:

- The separation bumps in the separation planes are collapsed synchronously in IP1 and 5.
- The separation bumps in the crossing plane are collapsed synchronously in IP1 and 5.
- The separation bumps in the separation plane in IP2 and 8 are reduced to the values requested for luminosity levelling in these two IPs.

The separation bumps in the crossing planes are not strictly required, nevertheless they are beneficial for the beam stability during the collision adjustment process [8, 39]. If they are not implemented, the time to collapse the separation bumps in the crossing plane from 2 σ full separation to 0 σ in IP1 and 5 should be less than 3 s to prevent the development of an instability. For IP2 and 8, there are no time constraints.

The optics parameters at the end of the collision adjustment process are shown in Table 13. The correction of dispersion generated by the crossing angle using orbit bumps in the arcs is not yet needed. It is assumed that this is switched on as the telescopic squeeze progresses. The IP2 and IP8 separation values are computed to provide the levelled luminosity as given in Table 12. The following aspects are taken into account in the estimate of the required octupole strength [8]:

- Latest machine impedance model, including the CCs high-order modes and the low impedance collimators [43, 44].
- Landau damping is computed for a Gaussian distribution with tails cut at 3σ in both transverse planes. The computations are based on the bunch intensity and transverse emittances listed in the corresponding tables. The potentially

Table 11: **Flat-top and collision adjustment process:** Collimation, injection protection and HEL settings. All collimator and injection protection settings correspond to the half-gap. Settings in σ correspond to a normalised emittance of 2.5μm. Both beams have the same value unless specified otherwise, blue for Beam 1 and red for Beam 2.

TCP/TCPM IR7 [σ]	8.5
TCSPM/TCSG IR7 [σ]	10.1
TCLA IR7 [σ]	13.7
TCLD IR2 [mm]	20
TCP IR3 [σ]	17.7
TCSG IR3 [σ]	21.3
TCLA IR3 [σ]	23.7
TCSP IR6 [σ]	11.1
TCSP IR6 (Beam 1 / Beam 2) [mm]	4.7 / 5.5
TCDQ IR6 [σ]	11.1
TCDQ IR6 (Beam 1 / Beam 2) [mm]	4.6 / 5.3
TCT H4-V4-H6-V6 IR1/5 [σ]	26.7-30.5-22.9-34.9 / 26.7-30.6-23.0-35.0 26.7-30.5-22.7-35.3 / 26.7-30.5-22.7-35.1
TCT H4-V4-H6-V6 IR1/5 [mm]	14.3-17.9-7.3-3.7 / 14.3-17.9-7.4-3.8 14.3-17.7-7.2-3.7 / 14.2-17.7-7.2-3.6
TCL4-5-6 IR1/5 [σ]	38.1-43.6-43.6 / 38.2-44.0-43.2 38.1-43.6-43.8 / 38.2-43.5-44.3
TCL4-5-6 IR1/5 [mm]	21.3-7.3-2.9 / 21.3-7.2-2.8 21.6-7.4-3.0 / 21.6-7.5-3.1
TCT IR2 [σ]	43.8
TCT IR8 [σ]	17.7
TDIS IR2 [mm]	55
TDIS IR8 [mm]	55
TCDD IR2 [mm]	42
TCLIA IR2 [mm]	29.5
TCLIA IR8 [mm]	28
TCLIB IR2 [mm]	28
TCLIB IR8 [mm]	28
Protected Aperture [σ]	20.4
HEL e^- beam current [A]	5
HEL e^- beam inner radius [σ]	6.5-7.5
HEL modulation pattern	Random ON/OFF (50 % ON)

beneficial impact of the second-order chromaticity is neglected. A stability diagram exceeding by a factor of 2 the instability threshold is required. This margin is based on empirical observations at the LHC in Run 2 and accounts for the uncertainty of the impedance model as well as for the impact of noise on the beam stability.

- H-V Tune separation larger than 5 times the low-intensity measured closest tune approach.
- Tune control within ± 0.001.
- Chromaticity control within ± 5 units.
- There should be enough margin with respect to the maximum strength of the Landau octupoles to compensate the possible detuning with amplitude caused by residual non-linearities after linear and non-linear optics correction.
- A maximum full separation error of 1σ in IP1 and 5 is reached at the end of the collision adjustment process

Figure 4 shows the DA at the end of the collision adjustment process, but pessimistically assuming the larger intensity of 2.3×10^{11} ppb and the lower emittance of 2 μm as it is not known when exactly the emittance growth happens plus DA is lower at 2 μm than at 2.5 μm. The DA of about 6σ is reached for few working points along the line $Q_y - Q_x = 0.005$, but without any margin. This is acceptable as IR non-linearities are still negligible at $\beta^* = 1$ m (after correction) and the time spent in this configuration with large Landau octupole current is in the order of minutes.

Additionally, the DA at this stage of the collision process can be further improved by reducing the octupole current. Stability studies have revealed the possibility of reducing the octupole current from 460 A to 400 A when considering an increased bunch length of 9 cm [31]. Although there is a mild sensitivity of the DA on the bunch length, the octupole reduction is expected to be beneficial for the DA.

Collimator, injection protection, and HEL settings are reported in Table 11.

7 Towards nominal luminosity levelling

Right after the collision adjustment process is performed, the beam stability of the colliding bunches is guaranteed by the beam-beam tune spread and the following actions should be performed while the detectors acquire luminosity data:

- The Landau octupole strength can start being reduced towards 80 A, once collisions are established in IP1 or IP5. This process may take a few minutes. The brightness of the witness bunches is assumed to be identical for

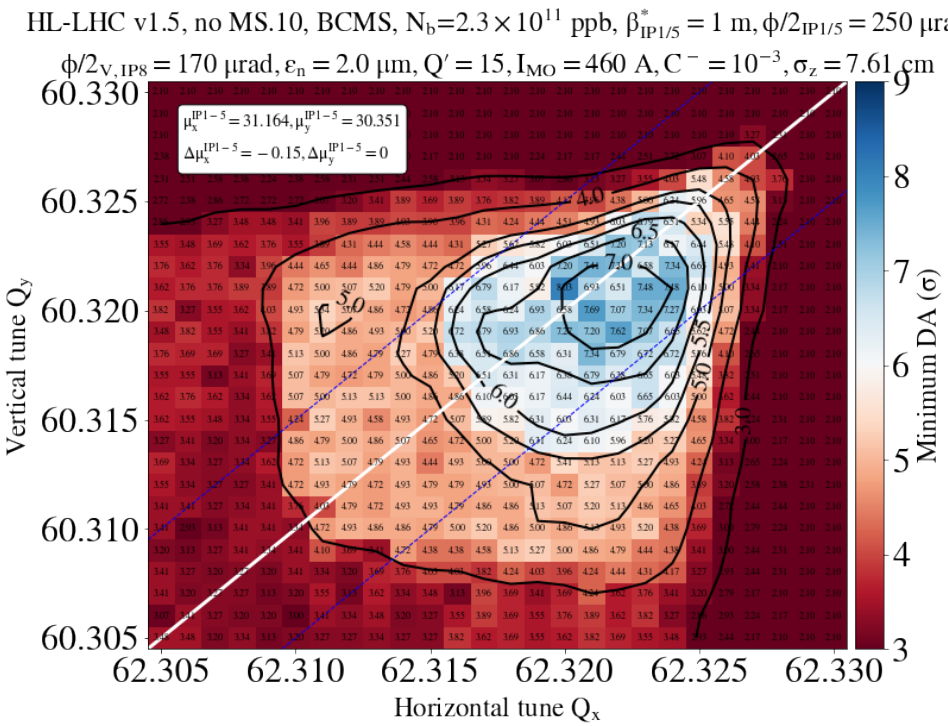

Figure 4: DA including beam-beam interactions at the end of the collision adjustment process versus horizontal and vertical tunes. A phase optimisation between IP1 and 5 is applied as $\Delta\phi_x$=−0.15, $\Delta\phi_y$=0. The normalised emittance of 2 μm and bunch intensity of 2.3×10^{11} ppb are pessimistically considered to allow for brighter beams.

Table 12: **Collision adjustment process:** Beam and luminosity parameters at the end of the collision adjustment process. RF parameters remain as in Table 9, except for the damper settings.

	Standard	BCMS
Energy [TeV]	7	
ppb [10^{11}]	2.2	
Particles per beam [10^{14}]	6.1	6.0
Beam current [A]	1.1	1.1
ε_n (H/V) [μm]	2.5	
ε_L [eVs]	3.03	
RMS bunch length (q-Gaussian) [cm]	7.61	
RMS energy spread (q-Gaussian) [10^{-4}]	1.1	
IBS growth-times (H/V/L) [h]	19.8/295/18.6	
Damping times from SR (H/V/L) [h]	51.7/51.7/25.9	
Power loss due to SR (per arc cell) [W/m/beam]	0.32	
Events/crossing μ in IP1/2/5/8	65/0.04/65/5.6	66/0.04/66/6.1
Peak pile-up density in IP1/2/5/8 [events/mm]	0.69/0.0003/0.69/0.05	
Luminosity in IP1/2/5/8 [10^{34}cm^{-2}s^{-1}]	2.5/0.0014/2.5/0.2	
Transverse damper damping time [turns]	10	
Transverse damper bandwidth [MHz]	10	

Table 13: **Collision adjustment process:** Optics and crossing scheme parameters at the end of the collision adjustment process. All separations and crossing angles correspond to the half of the distance between the two beams. The crossing angle and separation refer to Beam 1 if not specified otherwise. For Beam 2 the crossing angles and the separations have the opposite sign using the MAD-X Beam 1/Beam 2 reference system conventions. The half-separations in σ are estimated for the normalised emittance of 2.5 μm.

Optics filename	opt_adjust_1000
β^* [m] in IP1/2/5/8	1.0/10.0/1.0/1.5
ATS Telescopic factor r_{ATS}	1.0
Tunes (H/V)	62.317/60.322
Crossing angle at IP1 (ATLAS) [µrad]	250[e] (H)
Separation in separation plane at IP1 (ATLAS) [mm/σ]	0
Separation in crossing plane at IP1 (ATLAS) [mm/σ]	0
External crossing angle at IP2 (ALICE) [µrad]	-170[$] (V)
Crossing angle at IP2 (ALICE) [µrad]	$\mp$0.3 (H) $\mp$70-170 (V)
Separation in separation plane at IP2 (ALICE) [mm/σ]	0.13/2.34[i]
Separation in crossing plane at IP2 (ALICE) [mm]	0 (V)
External parallel angle at IP2 (ALICE) [µrad]	0 (H)
Crossing angle at IP5 (CMS) [µrad]	250[$] (V)
Separation in separation plane at IP5 (CMS) [mm/σ]	0 (H)
Separation in crossing plane at IP5 (CMS) [mm]	0 (V)
External crossing angle at IP8 (LHCb) [µrad]	170 (V)
Crossing angle at IP8 (LHCb) [µrad]	$\mp$135 (H) +170$\mp$1.8 (V)
Separation in separation plane at IP8 (LHCb) [mm/σ]	0.032/1.4[i] (H)
External parallel angle at IP8 (LHCb) [µrad]	0 (V)
Min. Landau octupole current (LOF) [A] required for beam stability (Standard/BCMS)	380 / 460
RMS betatron tune spread[j] [10^{-3}] (min/max, Standard ; BCMS)	0.06/2.5 ; 0.07/2.5
Residual detuning with amplitude due to lattice non-linearities [Amps-equiv. in LOF]	6

[e] In the horizontal plane the sign of the crossing angle is defined by the geometry.

[g] The other sign is possible. In the separation plane it is not correlated with other choices. In the crossing plane the same sign of the crossing angle is preferred for orbit corrector strengths.

[$] The other sign is possible.

[i] The other sign is possible but the parallel angle and separation are correlated for the same IP.

[j] Sources of detuning taken into account: Chromatic sextupoles, Landau octupoles, long-range and head-on beam-beam interactions.

Table 14: **Nominal levelling:** Luminosity and CCs parameters at the start of the nominal luminosity levelling. Beam and RF parameters remain as in Table 9.

	Standard	BCMS
Events/crossing μ in IP1/2/5/8	130/0.04/130/5.6	132/0.04/132/6.1
Peak pile-up density in IP1/2/5/8 [events/mm]	1.04/0.0003/1.04/0.05	
Luminosity in IP1/2/5/8 [10^{34}cm^{-2}s^{-1}]	5.0/0.0014/5.0/0.2	
CC voltage per cavity [MV]	3.4	
CC phase between cavities on same IP side [deg]	0	
CC total voltage [MV]	6.8	
CC crabbing angle [µrad]	$\pm$190	

the standard and BCMS beams (Sec. 2.1), therefore the octupole current is independent of the choice of beam type. The required octupole current can be scaled inversely linear to the achieved brightness of the witness bunches.

- The damper settings can be optimised to reduce the emittance-growth rate in collision (lower bandwidth and higher gain, see Table 12).
- Change the mode of operation of the HEL from Random ON/OFF (50 % ON) to N_{ON}=9 / N_{OFF}=5 or to DC mode, depending on the required tail depletion (to be assessed in Run 3).

To stay within cryogenics limitations, the luminosity should stay constant for about 10 minutes and then ramped up to nominal levelling values (see Table 14) in another 10 minutes. The luminosity ramp-up in IP1 and 5 is performed by ramping crab cavity voltage to 3.4 MV per cavity and reducing β^* to about 65 cm.

During these short periods, the beam, RF and collimator parameters remain very close to those at the end of the collision adjustment process (see Tables 12 and 11).

7.1 The first years of operation

As shown in Table 1 the first years of operation are foreseen to run without crab cavities and at a reduced bunch intensity of 1.7×10^{11} p. This allows to reduce the crossing angle to about 450 μrad as validated with the DA simulations in Fig. 5. It is foreseen to steadily reduce the crossing angle during the physics fill as bunch population decays to maximise performance.

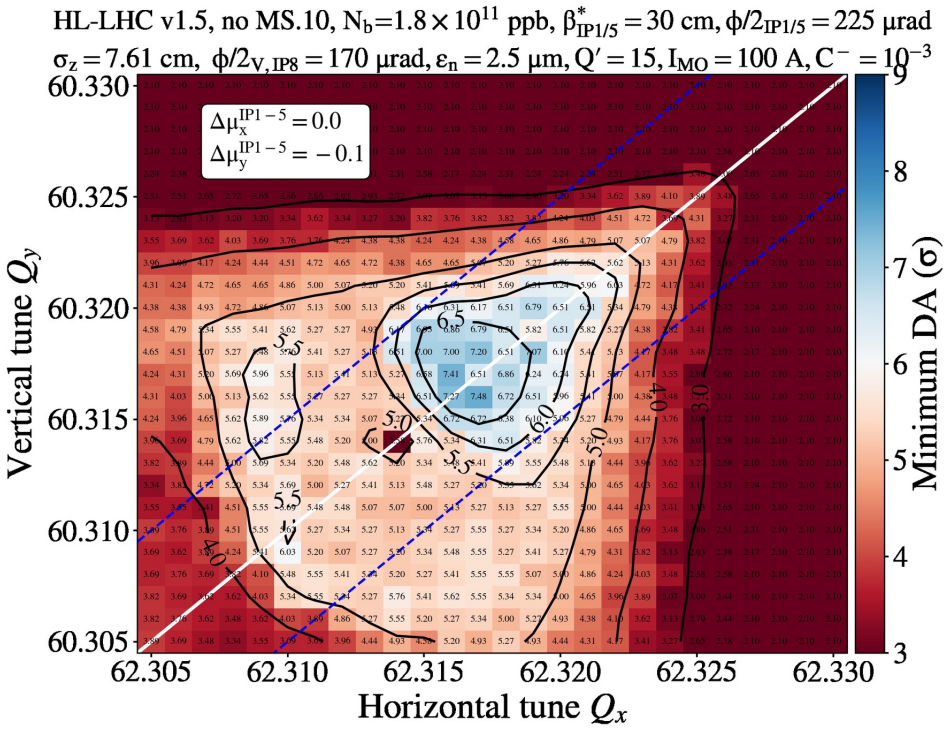

Figure 5: DA after the luminosity ramp-up in the first years of operation versus horizontal and vertical tunes including beam-beam interactions and for optimized phase advance between IP1 and IP5.

Table 15: **End of levelling:** Beam, luminosity and CCs parameters at the end of the luminosity levelling process. RF parameters remain as in Table 9.

	Standard	BCMS
Energy [TeV]	7	
ppb [10^{11}]	1.3	
Particles per beam [10^{14}]	3.588	3.567
Beam current [A]	0.646	0.642
ε_n (H/V) [μm]	2.9 / 2.2	
ε_L [eVs]	3.03	
RMS bunch length (q-Gaussian) [cm]	7.61	
RMS energy spread (q-Gaussian) [10^{-4}]	1.1	
IBS growth-times (H/V/L) [h]	33.3/2440/32.9	
Damping times from SR (H/V/L) [h]	51.7/51.7/25.9	
Power loss due to SR (per arc cell) [W/m/beam]	0.19	
Events/crossing μ in IP1/2/5/8	130/0.04/130/5.6	132/0.04/132/6.1
Peak pile-up density in IP1/2/5/8 [events/mm]	1.2/0.0003/1.2/0.05	
Luminosity in IP1/2/5/8 [10^{34}cm^{-2}s^{-1}]	5/0.0014/5/0.2	
CC voltage per cavity [MV]	3.4	
CC phase between cavities on same IP side [deg]	0	
CC total voltage [MV]	6.8	
CC crabbing angle [µrad]	$\pm$190	

8 End of luminosity levelling, $\beta^* = 20$ cm

During the luminosity-levelling phase, the β^* is reduced step-wise as burn-off reduces bunch population to keep the luminosity as constant as possible. In order to reduce the number of optics to be commissioned, it is possible to complement this β^* levelling with offset levelling in both IPs. However, it is also foreseen to use IP offsets to equalise luminosities in IP1 and 5. The offsets should respect the limit of 1 σ separation between the two beams to guarantee beam stability. The luminosity levelling at nominal luminosity should last for about 6 hours. The beam parameters at the end of luminosity levelling are shown in Table 15.

The optics parameters at the end of the luminosity levelling are shown in Table 16. It should be noted that both tunes have to be reduced by about 0.004 from the start of collisions to the end of levelling to ensure a good DA of 6 σ as shown in Fig. 6.

Table 16: **End of levelling:** Optics and crossing scheme parameters at the end of the levelling process. All separations and crossing angles correspond to the half of the distance between the two beams. The crossing angle and separation refer to Beam 1. For Beam 2 the crossing angles and the separations have the opposite sign using the MAD-X Beam 1/Beam 2 reference system conventions. The half-separations in σ are estimated for the normalised emittance of 2.5μm.

Optics filename	opt_coll_200
β^* [m] in IP1/2/5/8	0.2/10.0/0.2/1.5
ATS Telescopic factor r_{ATS}	2.5
Tunes (H/V)	62.313/60.318
Crossing angle at IP1 (ATLAS) [µrad]	250[e] (H)
Separation in separation plane at IP1 (ATLAS) [mm/σ]	0
Separation in crossing plane at IP1 (ATLAS) [mm/σ]	0
External crossing angle at IP2 (ALICE) [µrad]	-170[$] (V)
Crossing angle at IP2 (ALICE) [µrad]	$\mp$0.3 (H) $\mp$70-170 (V)
Separation in separation plane at IP2 (ALICE) [mm/σ]	0.11/1.8[i]
Separation in crossing plane at IP2 (ALICE) [mm]	0 (V)
External parallel angle at IP2 (ALICE) [µrad]	0 (H)
Crossing angle at IP5 (CMS) [µrad]	250[$] (V)
Separation in separation plane at IP5 (CMS) [mm/σ]	0 (H)
Separation in crossing plane at IP5 (CMS) [mm]	0 (V)
External crossing angle at IP8 (LHCb) [µrad]	170 (V)
Crossing angle at IP8 (LHCb) [µrad]	$\mp$135 (H) +170$\mp$1.8 (V)
Separation in separation plane at IP8 (LHCb) [mm/σ]	0.022/0.96[i] (H)
External parallel angle at IP8 (LHCb) [µrad]	0 (V)
Min. Landau octupole current (LOF) [A] required for beam stability	120
Max. LOF for good DA [A]	300
Residual detuning with amplitude due to lattice non-linearities [Amps-equiv. in LOF]	150
RMS betatron tune spread[j] [10^{-3}] (min/max, Standard ; BCMS)	0.03/1.3 ; 0.04/1.3

[e] In the horizontal plane the sign of the crossing angle is defined by the geometry.

[g] The other sign is possible. In the separation plane it is not correlated with other choices. In the crossing plane the same sign of the crossing angle is preferred for orbit corrector strengths.

[$] The other sign is possible.

[i] The other sign is possible but the parallel angle and separation are correlated for the same IP.

[j] Sources of detuning taken into account: Chromatic sextupoles, Landau octupoles, long-range and head-on beam-beam interactions

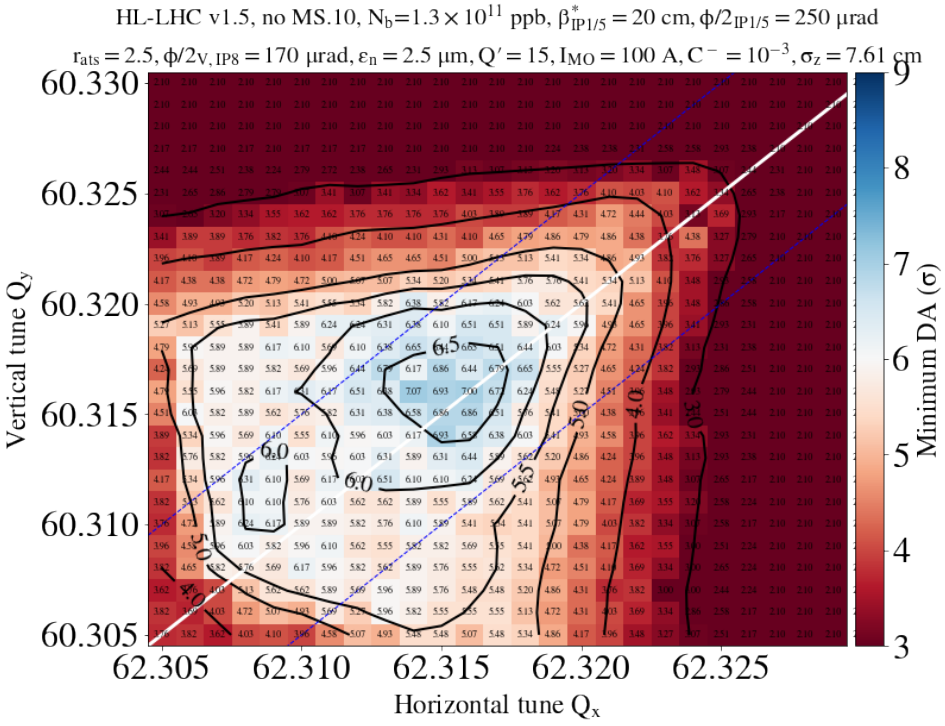

Figure 6: DA at the end of the luminosity levelling versus horizontal and vertical tunes including beam-beam interactions.

Table 17 shows the collimation, injection protection, and HEL settings at the end of the levelling process.

9 Potential limitations from Accelerating RF system

To accommodate the expected larger longitudinal emittance at SPS extraction with 2.3×10^{11} ppb, a minimum of 8 MV is required and up to a maximum of 8.8 MV maybe needed [40]. The maximum voltage corresponds to a steady-state RF power beyond the capability of the present system with the required half-detuning scheme. Acceptable capture losses, injection transients, SPS-LHC energy errors and line-by-line variations of the RF amplifiers may require additional margin. Taking these aspects into account, a minimum bunch intensity of 1.8×10^{11} ppb is estimated to be easily achievable. Further studies are ongoing to investigate the maximum bunch intensity feasible with the present RF system and whether an extra margin is required to reach the HL-LHC parameters in operation. Figure 7 shows the physics fill assuming an injected bunch charge of 1.8×10^{11} ppb. This lower bunch charge causes the fill to shorten by more than 2 hours and the leveling time by more than 3 hours with respect to the baseline shown in Fig. 2. The initial β^*_{start} is reduced to 45 cm. The integrated luminosity in a year with 160 days is reduced from 242 to 194 fb^{-1}, reducing the Run 4 expected integrated luminosity by about 20%. Figure 8 shows the yearly integrated luminosity versus bunch charge at injection in the range between 1.8×10^{11} ppb and the baseline value. One mitigation could be explored by reducing the crossing angle as there should be some margin from the lower bunch intensity.

10 Tune spread from Landau octupoles

The following proportionality relations can be used together with Table 18 to scale the detuning coefficients from the LHC Landau octupoles to any energy, r_{ATS} and

Table 17: **End of levelling:** Collimation, injection protection and HEL settings at the end of the levelling process. All collimator and injection protection settings correspond to the half-gap. Settings in σ correspond to a normalised emittance of 2.5 μm. Both beams have the same value unless specified otherwise, blue for Beam 1 and red for Beam 2.

TCP/TCPM IR7 [σ]	8.5
TCSPM/TCSG IR7 [σ]	10.1
TCLA IR7 [σ]	13.7
TCLD IR2 [mm]	20
TCP IR3 [σ]	17.7
TCSG IR3 [σ]	21.3
TCLA IR3 [σ]	23.7
TCSP IR6 [σ]	11.1
TCSP IR6 (Beam 1 / Beam 2) [mm]	4.8 / 4.7
TCDQ IR6 [σ]	11.1
TCDQ IR6 [mm]	4.6
TCT H4-V4-H6-V6 IR1&5 [σ]	13.2
TCT H4-V4-H6-V6 IR1/5 [mm]	14.3-17.9-7.3-3.7 / 14.3-17.9-7.4-3.8 14.3-17.7-7.2-3.7 / 14.2-17.7-7.2-3.6
TCL4-5-6 IR1&5 [σ]	16.4-16.4-16.3
TCL4-5-6 IR1/5 [mm]	21.3-7.3-2.9 / 21.3-7.2-2.8 21.6-7.4-3.0 / 21.6-7.5-3.1
TCT IR2 [σ]	43.8
TCT IR8 [σ]	17.7
TDIS IR2 [mm]	55
TDIS IR8 [mm]	55
TCDD IR2 [mm]	42
TCLIA IR2 [mm]	29.5
TCLIA IR8 [mm]	28
TCLIB IR2 [mm]	28
TCLIB IR8 [mm]	28
Protected aperture arcs [σ]	20.4
Protected aperture IR 1&5/2/8 [σ]	12.2-15.6 / 20.4 / 20.4
HEL e^- beam current [A]	5
HEL e^- beam inner radius [σ]	6.5
HEL modulation pattern	DC or N_{ON}=9 / N_{OFF}=5

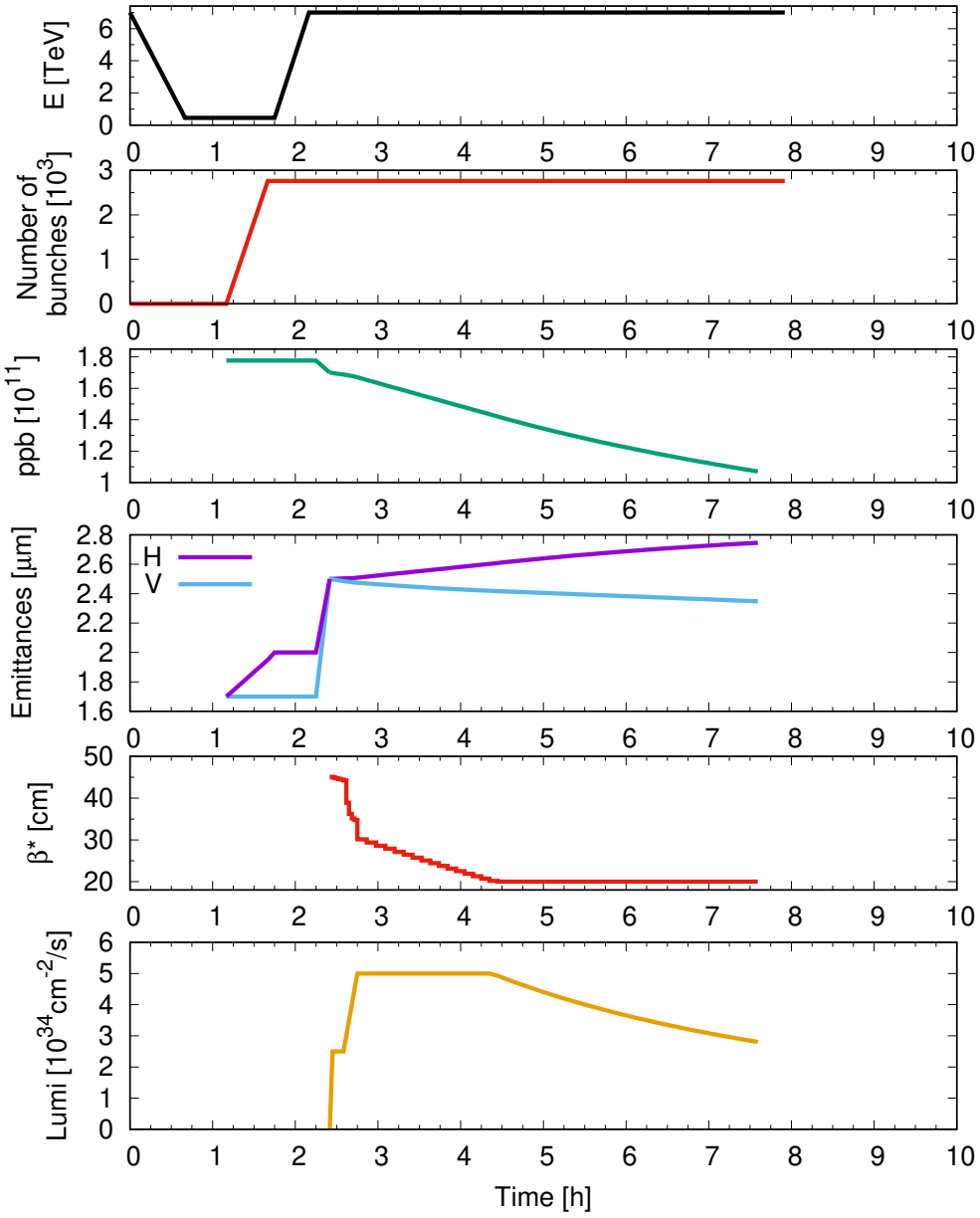

Figure 7: Same schematic view of the Run 4 HL-LHC physics cycle as in Fig. 2 but with an injection bunch charge of 1.8×10^{11} ppb.

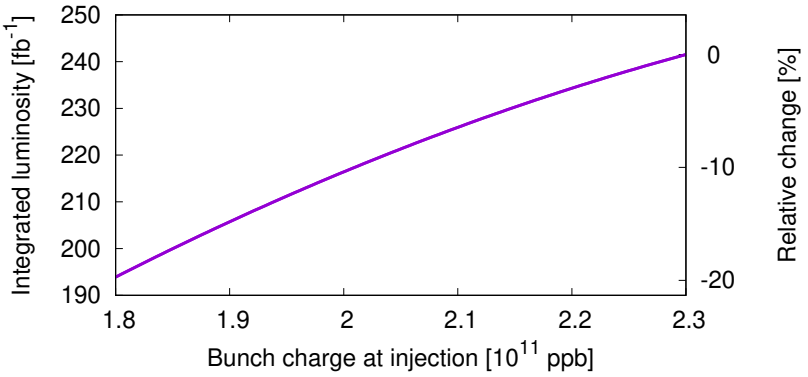

Figure 8: Yearly integrated luminosity versus bunch charge at injection in Run 4. A nominal year with 160 days for physics is assumed.

Table 18: Shift to amplitude detuning and second-order chromaticity from powering the Landau octupoles to 550 A at 7 TeV for three optics with different β^* and r_{ATS}. The rms tune spreads induced by the Landau octupoles are also given, computed as in Eqs. (7) with $\partial Q_{x,y}/\partial\delta_p = 0$. At 7 TeV $\sigma_\delta = 1.1\times10^{-4}$ and at 1 σ of the transverse distribution $2J = \varepsilon_n/\gamma = \varepsilon = 2.5\times10^{-6}/7463$ m.

	$\beta^* = 1$ m $r_{ATS} = 1$	$\beta^* = 0.20$ m $r_{ATS} = 2.5$	$\beta^* = 0.15$ m $r_{ATS} = 3.3$
$\frac{\partial Q_x}{\partial 2J_x}$ $[10^5\mathrm{m}^{-1}]$	1.4	2.9	4.6
$\frac{\partial Q_x}{\partial 2J_y}$ $[10^5\mathrm{m}^{-1}]$	-1.0	-1.5	-2.0
$\frac{\partial^2 Q_x}{\partial \delta_p^2}$ $[10^4]$	3.0	3.7	4.3
$\frac{\partial^2 Q_y}{\partial \delta_p^2}$ $[10^4]$	-1.2	-1.5	-1.8
$Q_{x,rms}$ $[10^{-4}]$	2.6	3.3	4.0
$Q_{y,rms}$ $[10^{-4}]$	1.2	1.7	2.3

octupole current [41]:

$$\frac{\partial Q_x}{\partial 2J_x} \approx \frac{\partial Q_y}{\partial 2J_y} \propto \frac{I_{MO}}{\gamma}\left(r_{ATS}+\frac{1}{r_{ATS}}\right)^2 \quad (3)$$

$$\frac{\partial Q_x}{\partial 2J_y} = \frac{\partial Q_y}{\partial 2J_x} \propto \frac{I_{MO}}{\gamma}\left(1+\frac{1}{4}\left(r_{ATS}+\frac{1}{r_{ATS}}\right)^2\right) \quad (4)$$

$$\frac{\partial^2 Q_x}{\partial \delta_p^2} \propto \frac{I_{MO}}{\gamma}\left(1+\frac{1}{4}\left(r_{ATS}+\frac{1}{r_{ATS}}\right)^2\right)^{\frac{1}{2}} \quad (5)$$

$$\frac{\partial^2 Q_y}{\partial \delta_p^2} \propto \frac{I_{MO}}{\gamma}\left(1+\frac{1}{4}\left(r_{ATS}+\frac{1}{r_{ATS}}\right)^2\right)^{\frac{1}{2}} . \quad (6)$$

The rms tune spread induced by the detuning terms is given by the following equations,

$$Q_{x,rms}^2 = \left(\frac{\partial Q_x}{\partial 2J_x}\right)^2 \varepsilon_x^2 + \left(\frac{\partial Q_x}{\partial 2J_y}\right)^2 \varepsilon_y^2 + \left(\frac{\partial Q_x}{\partial \delta_p}\right)^2 \sigma_\delta^2 + \frac{1}{2}\left(\frac{\partial^2 Q_x}{\partial \delta_p^2}\right)^2 \sigma_\delta^4$$

$$Q_{y,rms}^2 = \left(\frac{\partial Q_y}{\partial 2J_x}\right)^2 \varepsilon_x^2 + \left(\frac{\partial Q_y}{\partial 2J_y}\right)^2 \varepsilon_y^2 + \left(\frac{\partial Q_y}{\partial \delta_p}\right)^2 \sigma_\delta^2 + \frac{1}{2}\left(\frac{\partial^2 Q_y}{\partial \delta_p^2}\right)^2 \sigma_\delta^4 . \quad (7)$$

11 Outlook

A solid operational scenario has been established for the first run of the HL-LHC, Run 4. During the finalisation of this report modifications to the Run 3, LS3, Run 4 and in-kind contributions delivery schedules are being discussed that could impact parameter choices, as energy or bunch intensity, and hardware availability, as dispersion suppressor sextupoles or the HEL. The implications of the new configurations will be studied in the future.

Acknowledgments

We are very thankful to Stephane Fartoukh for helpful discussions on the Run 4 operational scenario. Research supported by the HL-LHC project.

References

[1] E. Métral *et al.*, "Update of the HL-LHC operational scenarios for proton operation", CERN-ACC-NOTE-2018-0002.

[2] F. Plassard *et al.*, "Sextupole scheme optimization for HL–LHC", CERN-ACC-NOTE-2021-0012.

[3] S. Kostoglou, "Review of the situation without MS10 at the beginning of collisions and at the end leveling", 189th HiLumi WP2 Meeting.

[4] P. Fessia *et al.*, "HL-LHC ECR - WP3/WP2/WP15 Deferral of Installation of Lattice Sextupole in Q10 in Points 1 and 5 to LS4", edms No. 2636486 v.0.5, ref. LHC-M-EC-0005 v.0.5.

[5] S. Claudet, "Request for slow luminosity increase", 160$^{\text{th}}$ HiLumi WP2 Meeting, September 2019.

[6] S. Claudet, "HL-LHC WP9 Cryogenics, Process studies, Coping with Peak Lumi (ramps)", 171$^{\text{st}}$ HiLumi WP2 Meeting, March 2020.

[7] E. Metral, "Impedance models, operational experience and expected limitations", International review of the LHC collimation system, CERN, 2019.

[8] X. Buffat *et al.*, "Strategy for Landau damping of head-tail instabilities at top energy in the HL-LHC", CERN-ACC-NOTE-2020-0059.

[9] F. Plassard *et al.* "Update on the DA studies at injection for HL-LHC", 168$^{\text{th}}$ HiLumi WP2 Meeting.

[10] S. Kostoglou *et al*, "Various DA studies with beambeam for HL-LHC", 194th HiLumi WP2 Meeting.

[11] Editors: I. Béjar Alonso, O. Brüning, P. Fessia, M. Lamont, L. Rossi, L. Tavian, M. Zerlauth, "High-Luminosity Large Hadron Collider (HL-LHC): Technical design report", CERN Yellow Reports: Monographs, Vol. **10** (2020).

[12] P. Baudrenghien, "News on feedback BPM specifications & update on emittance growth", Special Joint HiLumi WP2/WP4/WP13 Meeting, 15$^{\text{th}}$ June 2021.

[13] I. Efthymiopoulos, S.Kostoglou, G. Sterbini and R.Tomás, "Luminosity Performance Estimates in HL-LHC Run 4 and beyond - slightly flat optics?", in the 11th HL-LHC Collaboration Meeting, 2021.

[14] A. Herty, "HL-LHC full remote alignment study", 10th International Particle Accelerator Conference, Melbourne, Australia, 19 - 24 May 2019, THPGW057.

[15] R. Bruce *et al.*, "Functional Specification HELs - Functional and Operational Conditions", edms no. 2514085.

[16] Efthymiopoulos *et al.*, "LHCb Upgrades and operation at 10^{34} cm^{-2}s^{-1} luminosity – A first study", CERN-ACC-NOTE-2018-0038.

[17] N. Beev, M. Martino, M. Cerqueira Bastos, "Upgrade of the LHC class 1 power converter precision measurement systems: Class 0.5", EDMS No. 2379888.

[18] F. Carlier, *et al.*, "Optics Measurement and Correction Challenges for the HL-LHC", CERN-ACC-2017-0088.

[19] T. Pugnat, "Impact of non-linear correctors on DA for β^* =30 cm", Special Joint HiLumi WP2/WP4 Meeting, April 5, 2022.

[20] R. Tomás, J. Keintzel and S. Papadopoulou, "Emittance growth from luminosity burn-off in future hadron colliders", Phys. Rev. Accel. Beams **23**, 031002, March 2020.

[21] G. Iadarola, "Filling schemes update", 172th HL-LHC WP2 meeting.

[22] R. Tomás, I. Efthymiopoulos and G. Iadarola, "Burn-off with asymmetric interaction points, IPAC 2021.

[23] X. Buffat *et al.*, "HL-LHC Experiment Data Quality Working Group Summary Report", CERN-BE-2022-001.

[24] X. Buffat, "Stability of witness bunches", 191st HL-LHC WP2 meeting.

[25] P. Baudrenghien, "Input from RF on CC noise and high bandwidth BPM need", Special Joint HiLumi WP2/WP4 Meeting - Tuesday, 23 March 2021.

[26] https://lhc-optics.web.cern.ch/lhc-optics/HLLHCV1.5/scenarios/run4/

[27] L.R. Carver *et al.*, "Transverse beam instabilities in the presence of linear coupling in the Large Hadron Collider", Phys. Rev. Accel. Beams **21**, 044401.

[28] X. Buffat, *et al.*, "Optics measurement and correction strategies for HL-LHC", CERN-ACC-2022-0004.

[29] S. Papadopoulou *et al*, "Emittance growth in the LHC and impact on HL-LHC performance", 8th HL-LHC Collaboration Meeting, 2018.

[30] X. Buffat, "Impact of the longitudinal distribution on the transverse stability at flat top in the LHC", 234th HSC section meeting.

[31] N. Mounet and X. Buffat, "Impedance with the phase I collimation upgrade and mitigation with longer bunches", 199th HiLumi WP2 Meeting.

[32] S. Kostoglou and G. Sterbini, "DA at collisions as a function of bunch length", 199th HiLumi WP2 Meeting.

[33] https://lhc-beam-operation-committee.web.cern.ch/documents/Xing/Spectrometers-help.pptx

[34] O. Brüning, W. Herr and R. Ostojic, "A beam separation and collision scheme for IP2 and IP8 at the LHC for optics version 6.1", LHC Project Report 367.

[35] J. Dilly *et al.*, "Report and Analysis from LHC MD 3311: Amplitude detuning at end-of-squeeze", CERN-ACC-NOTE-2019-0042, March 2019.

[36] R. Bruce *et al.*, "Updated parameters for HL-LHC aperture calculations for proton beams", CERN-ACC-2017-0051.

[37] Luis Eduardo Medina Medrano *et al.*, "Assessment of the performance of High Luminosity LHC operational scenarios: integrated luminosity and effective pile-up density", Canadian Journal of Physics **97** (5), 498-508 (2018).

[38] R. Bruce *et al.*,"Principles for generation of time-dependent collimator settings during the LHC cycle", CERN-ATS-2011-114.

[39] X. Buffat , "The mode coupling instability with offset beams", 23rd ABP-CEI Section Meeting, 2021.

[40] H. Timko et al., "LHC injection loss studies and power limit update" 11$^{\text{th}}$ HL-LHC Collaboration meeting 2021.

[41] S. Fartoukh, N. Karastathis, L. Ponce, M. Solfaroli and R. Tomás, "About flat telescopic optics for the future operation of the LHC", CERN-ACC-2018-0018.

[42] HL-LHC Technical Coordination Committee Parameter Table.

[43] N. Mounet, *et al.*, "Update on the HL-LHC impedance model in the new operational scenario and considerations on crab cavity HOMs," 179$^{\text{th}}$ HL-LHC WP2 Meeting

[44] https://impedance.web.cern.ch/